

Ignition kernel statistics of Delft Jet-in-Hot Coflow flames

E. Oldenhof*, M.J. Tummers, E.H. van Veen, D.J.E.M. Roekaerts

Department of Multi-Scale Physics, Delft University of Technology, Lorentzweg 1 2628 CJ Delft, The Netherlands

Abstract

The stabilization region of diffusion flames of natural gas in a hot, oxygen-lean coflow generated by the Delft Jet-in-hot-Coflow (DJHC) burner was studied using an intensified high-speed camera. Analysis of the resulting frames showed that auto-ignition is the dominant mechanism stabilizing the flame. Ignition kernels are formed randomly and are convected downstream while growing in size and connecting to other kernels. The statistics of these processes were studied, showing that ignition probabilities become larger for larger coflow temperatures. No strong influence of coflow temperature on flame propagation speeds is found. A simple mathematical model in 1-D is proposed, describing the probability of finding a burning flame at a certain axial location as function of ignition probabilities and flame propagation speed.

Introduction

Flameless combustion has strong advantages over conventional combustion, such as high efficiencies and low NO_x emissions [1]. As chemistry in these low-temperature flames is slow, turbulence-chemistry interaction is stronger thus making modelling of flameless combustion challenging. One of the modelling challenges lies in the prediction of lift-off height and flame stabilization [2]. Recently, the formation of ignition kernels in flames in a hot vitiated coflow was studied using advanced planar laser-diagnostic measurements [3]. In this work the frequently used concept of lift-off height has been investigated for flames in a hot coflow, in a statistical manner rather than in an average sense. Making use of a boundary-detection algorithm in matlab, statistics on ignition kernel formation and growth were analyzed. A 1-D approach was chosen, to avoid complications caused by line-of-sight effects.

Research objectives

The goal of this work is to quantify the concept of lift-off height for several Jet-in-Hot-Coflow flames in a statistical manner and to describe the relevant physical mechanisms.

Experimental setup

The DJHC burner, described in [4], is designed to deliver a flame that mimics the important characteristics of flameless combustion. It creates a turbulent diffusion flame of natural gas in a coflowing oxidizer stream of high temperature carrying little oxygen. The design is similar to the Adelaide JHC burner [5] and is illustrated in figure 1. A range of different flames is studied, differing in coflow temperature, coflow mixture fraction and in jet Reynolds numbers. The resulting flame structure between $x = 0$ mm (the location of the fuel jet exit) and $x = 180$ mm is studied with a Lambert Instruments HI-CR intensified camera, at a resolution of 1280x256 pixels and a framerate of 2000 fps. Calibration of the coordinates corresponding to pixel locations was done for each series, using a metal screen with square holes. A dark screen was placed behind the burner to minimize background signal. A Tamron zoom lens was used, at $f \approx 100$ mm.

*Corresponding author: E.Oldenhof@tudelft.nl
Proceedings of the European Combustion Meeting 2009

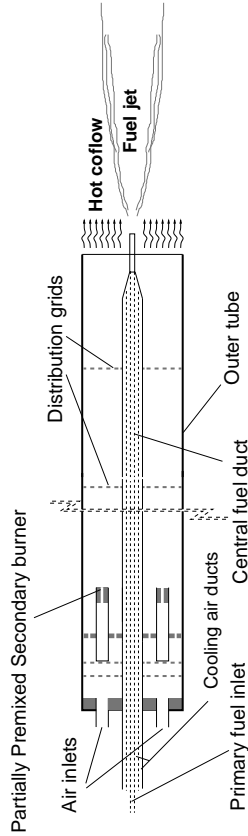


Figure 1: Conceptual design of the Delft JHC burner

Case description

The DJHC burner allows variations in coflow mixture fraction, influencing both coflow temperature and oxygen level. Furthermore, the amount of heat loss can be varied by using either one or two distribution grids, influencing only coflow temperature, see figure 2. Table 1 lists the characteristics of the different flames that were considered in this study. The roman letter in the case name denotes the variation in coflow mixture fraction, while the one- or two grid configurations are distinguished by the letter S (single grid) and D (double grid). Only single grid configurations are studied here. The temperature profiles were measured for the DJHC-I.S and DJHC-X.S cases only. The cases in between (from DJHC-II.S to DJHC-IX.S) are linearly interpolated in terms of mixture fraction (secondary burner mass flows). The temperature in the coflow is not constant but depends strongly on radial location as can be seen in figure 2. To characterize the coflow temperature, the maximum temperature is chosen as parameter.

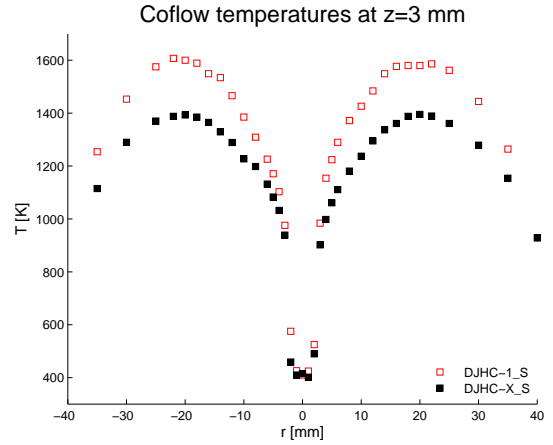


Figure 2: Temperatures as determined with CARS in DJHC-1.S and DJHC-X.S flames

Case	gas [nl/min]	air [nl/min]	$T_{\max;co}$ [K]	$Y_{O_2;co}$ -
DJHC-I.S	16.10	224	1607	8.41%
DJHC-II.S	15.89	225.7	^a	8.68%
DJHC-III.S	15.68	227.3	^a	8.95%
DJHC-IV.S	15.47	229.0	^a	9.22%
DJHC-V.S	15.26	230.7	^a	9.49%
DJHC-VI.S	15.04	232.3	^a	9.76%
DJHC-VII.S	14.83	234.0	^a	10.03%
DJHC-VIII.S	14.62	235.7	^a	10.30%
DJHC-IX.S	14.41	237.3	^a	10.57%
DJHC-X.S	14.20	239.0	1395	10.84%

^a not measured

Table 1: Secondary burner flows and resulting coflow characteristics of the studied DJHC flames

Image processing

Procedure

For each flame, 10,000 frames are shot at a frame-rate of 2000 fps, corresponding to an averaging time of 5 seconds. A background image is subtracted from each frame, which is constructed by averaging over 500 frames with identical exposure times and intensification, but without the presence of a flame. A circular averaging filter with a radius of 8 pixels is applied to reduce the influence of noise, after which the boundaries are determined based on a certain threshold level. To construct the flame probabilities as function of axial distance, the boundaries are analyzed in a separate routine, deciding for each frame whether each

row of pixels in radial direction contains a burning pocket or not. For each pixel row, the number of images where a burning pocket is found is divided by the total number of images, producing a ‘flame probability’ P_b . An instantaneous snapshot with the identified boundaries of the pockets is shown in figure 3. To determine the speeds of front and trailing ends of flame pockets, an algorithm is used that, based on the flame boundary locations at time t and those at time $t + 1$, decides whether the flame boundaries at $t + 1$ are new (an ignition event) or originate from an existing pocket at time t . In the latter case, the increment is recognized as either a front edge or trailing edge increment, and the location corresponding to the increment is linearly interpolated between those at the two consecutive times. Only forward movements are allowed, which, considering the histograms of velocities, seems to be an appropriate choice: the pdf of increment is always bell shaped with a maximum for positive increments. To decide which front and trailing edge at t corresponds to those at $t + 1$, the ‘best candidate’ is selected, i.e. the front and trailing edges at t with the shortest increment in forward direction. If no such candidate is found, the front is considered to originate from an ignition event, located at the trailing edge of the flame pocket at $t + 1$.

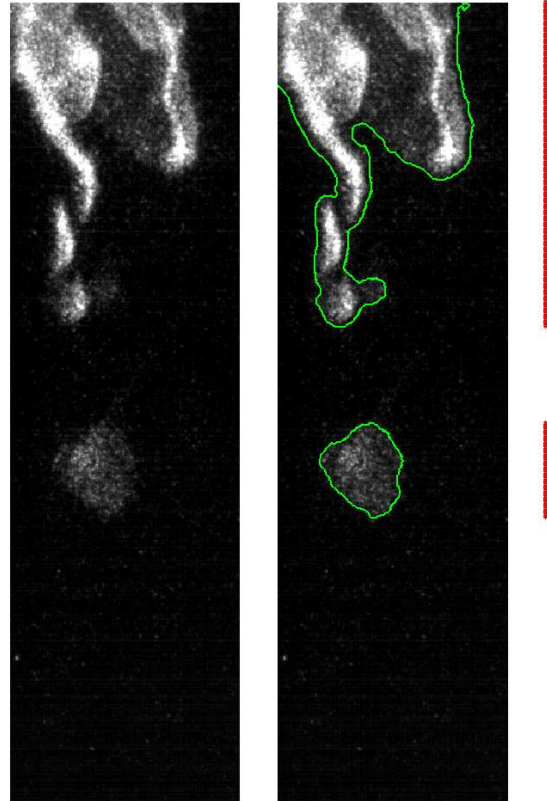


Figure 3: *Original frame, with subtraction of background (left), frame with flame boundary as determined by the matlab algorithm (middle) and the red line denoting the eventually used information: the axial location of flame-fronts. The jet direction is from bottom to top*

Sensitivity study of threshold intensities

Certain cases have been studied with a range of threshold intensities, to investigate the sensitivity of the flame probability P_b on this parameter. Levels are chosen by visual inspection, the highest level is such that ignition kernels are occasionally ignored in their developing stage, at the lowest level bad frame-to-frame correlation (misidentified kernels) becomes evident. Results are displayed in figure 4. The influence of chosen threshold level is modest, compared to differences between cases.

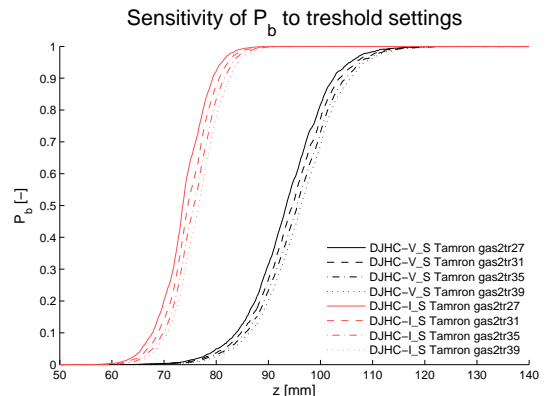


Figure 4: *Sensitivity of flame probabilities to intensity threshold levels*

Results and discussion

Observations on the flame probability

The dependence of the flame probability, P_b , on coflow temperature is strong, as shown in figure 5. The location where P_b starts to rise increases with decreasing coflow temperature, the gradient of P_b with respect to axial location decreases with decreasing coflow temperature. It will be shown in the following sections that this is related to changing ignition probabilities. The Reynolds number of the jet also influences the lift-off height, but in a reverse direction as normally seen in diffusion flames: higher jet velocities shift the curve of P_b toward the jet nozzle, figure 6.

Observations on the ignition probability

By counting ignition events, defined as those events where trailing edges do not originate from those at upstream locations at a previous timestep as described earlier, ignition probabilities per time per axial length can be calculated. Actually, the measured probability is different from the true ignition probability, since it can only be measured when no flame is present at the axial location. Assuming statistical independence of flame presence at an axial location and ignition probability, the following expression relates true and measured probabilities, the latter indicated with an asterisk: $P_{\text{ign}} = P_{\text{ign}}^*(1 - P_b)$. It appears that increasing the coflow temperature leads to have strongly increased ignition probabilities, at earlier locations. As an example, the ignition probabilities for the cases DJHC-LS and DJHC-V_S are shown in figure 7.

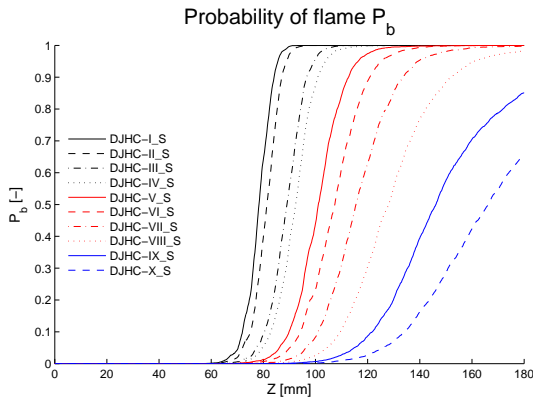


Figure 5: P_b as function of axial distance z for cases DJHC-LS to DJHC-X_S

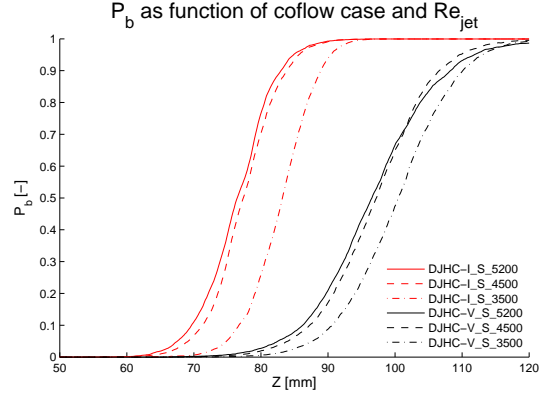


Figure 6: P_b as function of axial distance z for cases DJHC-LS and DJHC-V_S and different jet Reynolds numbers

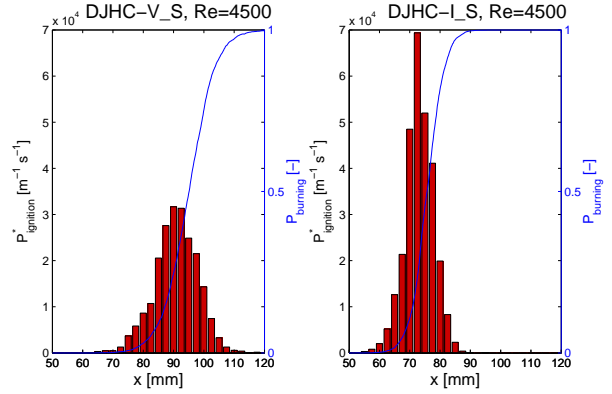


Figure 7: P_{ign}^* and P_b as function of axial distance z for cases DJHC-LS and DJHC-V_S, $Re=4500$

Observations on the flame propagation speeds

Following the procedure as described previously, velocities of front- and trailing edges of different flames were determined. The average (in case of front speeds) and the mode (the most likely velocity) in case of trailing edge speeds are shown in figure 8, for the DJHC-LS and DJHC-V_S flames, each for three different jet Reynolds numbers. The reason for taking the mode value instead of the average for trailing edges, is that the pdf of velocities is non-zero at $v = 0$ m/s, leading to a cut-off. The non-zero value is attributed to the fact that auto-ignition takes place throughout a certain volume, leading to apparent propagation velocities at early stages. A most distinctive feature of figure 8 is the fact that these velocities are hardly influenced by either the Reynolds number or the coflow temper-

ature. This suggests that the mechanism of ignition, growth and transport of kernels is dominant in all flames, not just in the low temperature cases where individual kernel formation is more visually apparent. The independence of the mean of the propagation velocities -which would be equal to the convective velocity for equal front and trailing edge velocities- is explained by the fact that the flame resides in the outer regions of the jet. The velocity at $z = 120$ mm at the mean location of the flame ($r = 17$ mm) has been determined by LDA measurements to be around 5 m/s, which is indeed halfway the front and trailing edge velocity.

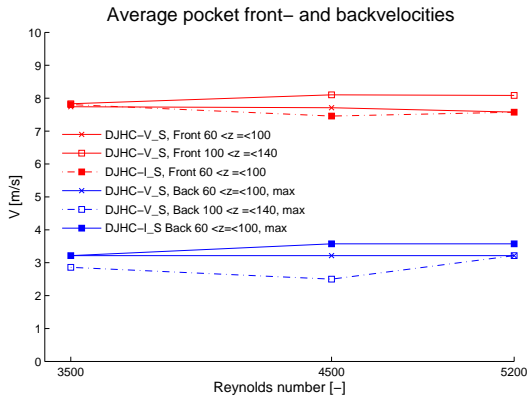


Figure 8: *Front and trailing edge velocities, cases DJHC-I,S and DJHC-V,S, three Reynolds numbers*

Relation between ignition and flame pocket probabilities

The flame probability is obviously related to ignition probabilities in an integral sense. Because pockets will grow in size, the probability of finding a burning pocket at a certain point is a function of ignition probabilities up to that point and the growth speed of the pockets. In the derivation of the relation between ignition and flame pocket probabilities, a non-stochastic pocket propagation speed is assumed. The probability of finding a burning pocket at axial location z , $P_b(z, t)$ is determined by the integral of probability of the formation of an ignition kernel per unit time and axial distance $P_{ign}(z)$ over the area in (z, t) -space where a kernel will reach this location:

$$P_b(x^*) = 1 - \exp \left[-\Phi \int_{x=0}^{x=x^*} (x^* - x) P_{ign}(x) dx \right] \quad (1)$$

where Φ is related to the pocket propagation speed:

$$\Phi = \frac{1}{v_{back}} - \frac{1}{v_{front}} = \frac{2V_0}{V_0^2 - V_f^2} \quad (2)$$

with V_0 the fluid velocity and V_f the flame propagation velocity, taken identical in the front and the back of the pocket.

Conclusions

For all studied flames (DJHC-I,S to DJHC-X,S), the mechanisms determining the average flame location, or “lift-off height”, are not the upstream propagation of a flame front, but the random process of auto-ignition and subsequent growth and downstream transport. The probabilities of auto-ignition increase for hotter coflows and shift downward. The average values of propagation speeds are hardly dependent on coflow temperature or jet Reynolds number. The latter is explained by the fact that the flame resides in a region most affected by coflow velocities. The decreasing lift-off heights for increasing Reynolds numbers is not caused by different propagation speeds or higher probabilities of ignition, but more probably due to the shortening of the potential core of the jet for higher Reynolds numbers.

Acknowledgements

The authors would like to thank Technology Foundation STW for their financial support.

Derivation of the dependence of P_b on P_{ign} and propagation speeds

In the general case of random propagation speeds of the front and trailing edges of flame pockets, the flame probability $P_b(x^*)$ is determined by an integral involving ignition probabilities $P_{ign}(x)$ and the transition probabilities $P_{tr}(\Delta x^*, \Delta t)$. The latter denotes the probability of a kernel, with origin (x, t) to be some time Δt later in the location $x + \Delta x^*$. Written as a convolution, and taking constant P_{tr} for all locations,

$$P_b(x^*) = 1 - \exp [- P_{ign}(x) * P_{tr}(\Delta x^*, \Delta t)] \quad (3)$$

The transition probability is itself an integral property, determined by integration over the joint PDF of front and trailing edge increments. For a flame front to be present at x^* , the trailing edge must be behind and the front edge in front of x^* :

$$P_{tr}(\Delta x^*, \Delta t) = \int_{-\infty}^{\Delta x^*} \int_{\Delta x^*}^{\infty} P_{(\Delta x_b, \Delta x_f)}(\Delta t) d\Delta x_f d\Delta x_b \quad (4)$$

In case of fixed front and trailing pocket edge speeds, the increment pdf

$$P_{\Delta x_b, \Delta x_f}(\Delta t) = \delta(\Delta t v_b) \delta(\Delta t v_f) \quad (5)$$

and the transition probability

$$P_{tr}(\Delta x^*, \Delta t) = \begin{cases} 1 & \text{if } \Delta t v_b \leq \Delta x^* < \Delta t v_f \\ 0 & \text{otherwise} \end{cases} \quad (6)$$

resulting in the following equation:

$$\begin{aligned} P_b(x^*) &= \\ 1 - \exp &\left[- \int_{x=0}^{x=x^*} \int_{(x^*-x)/v_f}^{(x^*-x)/v_b} P_{ign}(x) d\Delta t dx \right] \\ &= 1 - \exp \left[-\Phi \int_{x=0}^{x=x^*} (x^* - x) P_{ign}(x) dx \right] \end{aligned} \quad (7)$$

which is equivalent to equation 1, because of time invariance in the time integral boundaries.

For general $P_{\Delta x_f, \Delta x_b}(\Delta t)$, the boundaries of P_{tr} are not sharp. To see the influence of random propagation speeds, the integral of P_{tr} over Δx is evaluated. Using the function

$$\begin{aligned} \Psi(x, y) &= \\ &\int_{-\infty}^{\infty} \int_{-\infty}^{\Delta x^*} \int_{\Delta x^*}^{\infty} \delta(x) \delta(y) dx dy d\Delta x^* \\ &= y - x \end{aligned} \quad (8)$$

excluding the region $\Delta x_f < \Delta x_f$ - corresponding to the event of pocket disappearance - and using equation 4

$$\begin{aligned} \int_{-\infty}^{\infty} P_{tr} d\Delta x^* &= \\ &\iint \Psi(\Delta x_b, \Delta x_f) P_{\Delta x_f, \Delta x_b} d\Delta x_f d\Delta x_b \\ &= \Psi(\overline{\Delta x_b}, \overline{\Delta x_f}) = \overline{\Delta x_f} - \overline{\Delta x_b} \\ &= \Delta t (\overline{v_f} - \overline{v_b}) \end{aligned} \quad (9)$$

using the fact that Ψ is a linear function and that $P_{\Delta x_f, \Delta x_b}$ is a pdf. Thus, the transition probability integrated over Δx is only a function of the average pocket propagation velocities, random pocket propagation velocities will smear out P_{tr} horizontally.

References

- [1] J. A. Wunning and J. G. Wunning. Flameless oxidation to reduce thermal no-formation. *Progress in energy and combustion science*, 23(1):81–94, 1997.
- [2] S. Kumar, P. J. Paul, and H. S. Mukunda. Prediction of flame liftoff height of diffusion/partially premixed jet flames and modeling of mild combustion burners. *Combustion Science and Technology*, 179:2219–2253, 2007.
- [3] R. L. Gordon, A. R. Masri, and E. Mastorakos. Simultaneous rayleigh temperature, oh- and ch2o-lif imaging of methane jets in a vitiated coflow. *Combustion and Flame*, 155:181–95, 2008.
- [4] E. Oldenhof, M.J. Tummers, E.H. van Veen, and D.J.E.M. Roekaerts. The turbulent flowfield of the delft jet-in-hot-coflow burner. *Proceedings of the 5th European Thermal-Sciences Conference, May 2008, Eindhoven*, page 61, 2008.
- [5] B. B. Dally, A. N. Karpetsis, and R. S. Barlow. Structure of turbulent non-premixed jet flames in a diluted hot coflow. *Proceedings of the combustion institute*, 29:1147–1154, 2003.